Irreversible Growth of a Binary Mixture Confined in a Thin Film Geometry with Competing Walls

Julián Candia and Ezequiel V. Albano

Instituto de Investigaciones Fisicoquímicas Teóricas y Aplicadas (INIFTA), UNLP, CONICET, Casilla de Correo 16, Sucursal 4, (1900) La Plata, Argentina

(Received 5 September 2001; published 19 December 2001)

The irreversible growth of a binary mixture under far-from-equilibrium conditions is studied in three-dimensional confined geometries of size $L_x \times L_y \times L_z$, where $L_z \gg L_x = L_y$ is the growing direction. A competing situation where two opposite surfaces prefer different species of the mixture is analyzed. Because of this antisymmetric condition, an interface between the different species develops along the growing direction. Such interface undergoes a localization-delocalization transition that is the precursor of a wetting transition in the thermodynamic limit. Furthermore, the growing interface also undergoes a concave-convex transition in the growth mode. So, the system exhibits a multicritical wetting point.

DOI: 10.1103/PhysRevLett.88.016103 PACS numbers: 64.60.Cn, 05.50.+q, 68.35.Rh

The study of interfacial phenomena of materials confined in thin film geometries under equilibrium conditions has drawn enormous attention over the past few decades [1–3]. Interfacial phase transitions and critical phenomena in confined samples exhibit a quite distinct physical behavior compared to that occurring in the bulk due to the finite separation between the walls and the specific wall-particle interaction [1]. The understanding of this new type of phenomena is not only of general and fundamental interest but may also play an important role in the development of new technologies. Accordingly, the properties of films of magnetic materials [4–7], polymer blends [8,9], binary mixtures [10], fluids [11], etc., have been investigated thoroughly. Liquid-gas condensation under confinement between identical walls displays capillary condensation when the walls promote the fluid phase [12]. Mapping the fluid into a lattice gas model and using the magnetic terminology, the wall-particle interaction is accounted for by a surface magnetic field [4–7]. For this reason, Ising-like models are very useful to understand the underlying physics of more complex systems [13]. Another interesting scenario takes place when an Ising film is confined between two competing walls a distance L apart from each other, so that the surface magnetic fields (H) are of the same magnitude but opposite direction. These competing fields cause the emergence of an interface that undergoes a localization-delocalization transition at an L-dependent temperature $T_w(L, H)$ that is the precursor of the true wetting transition temperature $T_w(H)$ of the infinite system.

It is surprising that, in contrast to the effort devoted to the understanding of wetting phenomena under equilibrium conditions, the nonequilibrium counterpart has received very little attention. For instance, Hinrichsen*et al.* [14] have introduced a nonequilibrium growth model of a one-dimensional interface that undergoes a transition from a bounded state to a nonbounded one.

Within this context, the aim of this work is to perform an extensive numerical study of the irreversible growth of a magnetic material confined between parallel walls where competing surface magnetic fields act. It is shown that the interplay between confinement and growth mode leads to a physically rich phase diagram (on the plane H-T) that exhibits a localization-delocalization transition in the interface that runs along the walls and a change of the curvature of the growing interface running perpendicular to the walls. Extrapolation of this scenario to the thermodynamic limit leads to a multicritical wetting point.

The growth of a ferromagnetic material, with spins having two possible orientations, is studied using the so-called magnetic Eden model (MEM) [15]. Monte Carlo simulations are performed on the square lattice in $(2 + 1)$ dimensions, using a rectangular geometry $L_x \times L_y \times L_z$ with $L_z \gg L_x = L_y = L$. The location of each site on the lattice is specified through its rectangular coordinates (i, j, k), $(1 \le i, j \le L,\ 1 \le k \le L_z)$. The starting seed for the growing cluster is a plane of $L \times L$ spins placed at $k = 1$, and cluster growth takes place along the positive longitudinal direction (i.e., $k \ge 2$). The boundary conditions are periodic along one of the transverse directions (for example, in the i direction) but open along the remaining transverse direction. In the latter, competing surface magnetic fields $H_1 > 0$ ($H_L < 0$) acting on the sites placed at $j = 1$ ($j = L$), with $H = H_1 = |H_L|$, are considered. Then, clusters are grown by selectively adding spins ($S_{ijk} = \pm 1$) to perimeter sites, which are defined as the nearest-neighbor (NN) empty sites of the already occupied ones.

Considering a ferromagnetic interaction of strength $J > 0$ between NN spins, the energy E of a given configuration of spins is given by

$$E = -\frac{J}{2}\left(\sum_{\langle ijk,i'j'k'\rangle} S_{ijk}S_{i'j'k'}\right) - H\left(\sum_{\langle ik,\Sigma_1\rangle} S_{i1k} - \sum_{\langle ik,\Sigma_L\rangle} S_{iLk}\right), \qquad (1)$$

where the summation $\langle ijk, i'j'k' \rangle$ is taken over occupied NN sites, while $\langle ik, \Sigma_1 \rangle$, $\langle ik, \Sigma_L \rangle$ denote summations carried over occupied sites on the surfaces $j = 1$ and $j = L$, respectively. Throughout this work, we set the Boltzmann constant equal to unity and we take the temperature, energy, and magnetic fields measured in units of J. The probability for a perimeter site to be occupied by a spin is taken to be proportional to the Boltzmann factor $\exp(-\frac{\Delta E}{T})$, where ΔE is the change of energy involved in the addition of the given spin. At each step, the probabilities of adding up and down spins to a given site have to be evaluated for all perimeter sites. After proper normalization of the probabilities, the growing site and the orientation of the spin are determined with Monte Carlo techniques. Using this procedure, clusters having up to 10^9 spins have typically been grown. Although both the interaction energy and the Boltzmann probability distribution considered for the MEM are similar to those used for the Ising model with surface magnetic fields [9,12], it must be stressed that these two models operate under extremely different conditions, namely, the MEM describes the irreversible growth of a magnetic material and the Ising model deals with a magnet under equilibrium. Previous studies have demonstrated that the MEM in $(1 + 1)$ dimensions is not critical but it exhibits a second-order transition at $T_c = 0.69 \pm 0.01$ in $(2 + 1)$ dimensions [16].

The phase diagram of the MEM in a confined geometry with competing surface fields is very rich and exhibits eight regions. For the sake of clarity, we will first discuss the main characteristics of each of these regions by means of snapshot configurations (see Fig. 1). Subsequently, we will quantitatively locate the boundary between these regions and plot the corresponding phase diagram (see Fig. 2). Finally, we will draw the phase diagram in the thermodynamic limit (see inset of Fig. 2) by extrapolating finite-size results (see Fig. 3).

The vertical straight line at $T_c(L = 12) = 0.84$ (see Fig. 2) represents the L-dependent "critical" temperature of the finite system [17]. So, the left(right)-hand side part of the phase diagram corresponds to the ordered (disordered) growth regime that involves Regions I, II, III, IV, and A (Regions V, VI, and B).

For low temperatures and small fields [Region I of Fig. 2, see also Fig. 1(a)], the system grows in an ordered state and a domain having mostly spins with a single orientation prevails. Because of thermal fluctuations, small clusters with the opposite orientation may appear, preferably on the surface where the field competing with the dominant orientation is applied. These "drops" might grow and, when the typical size of the fluctuation is of the order of L, a magnetization reversal may occur, thus changing the sign of the dominant domain. The formation of sequences of well ordered domains is a finite-size effect that is also characteristic of the ordered phase of some confined spin systems such as the Ising magnet [7]. Because of the open boundary conditions, empty perimeter sites at the confinement walls experience a missing neighbor effect. Since H is too weak to compensate this effect, the system grows preferentially along the center of the sample as compared to the walls, and the resulting growth interface exhibits a convex shape. So, Region I corresponds to the Ising-like nonwet state and the convex growth regime.

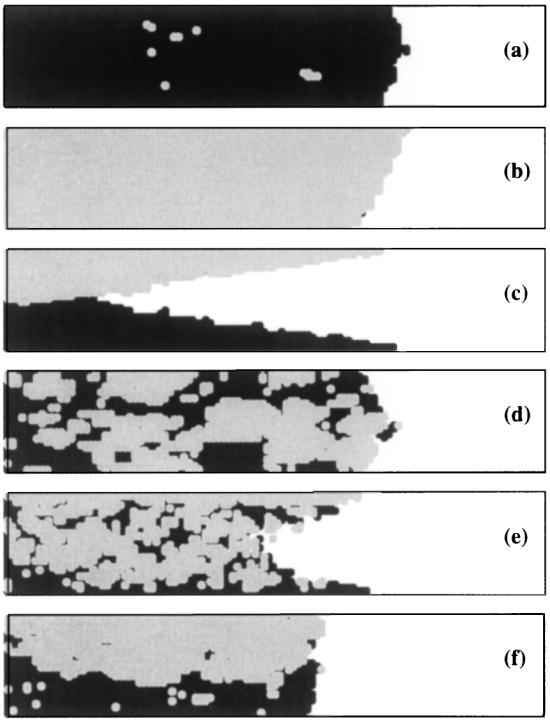

FIG. 1. Snapshot pictures showing a longitudinal slice given by a fixed value of the transverse coordinate i. Gray (black) circles correspond to spins up (down). The surface field on the upper (lower) confinement wall is positive (negative). The snapshots correspond to a lattice size $L = 32$ and several different values of temperature and surface fields: (a) $H = 0.05$, $T = 0.6$; (b) $H = 0.5$, $T = 0.55$; (c) $H = 1.4$, $T = 0.6$; (d) $H = 0.1$, $T = 1.0$; (e) $H = 1.6$, $T = 1.4$; and (f) $H = 0.20$, $T = 0.82$.

Increasing the field but keeping the temperature low enough, one may enter Region II (Fig. 2, see also Fig. 1(b)]. Here the system is still in its ordered phase and neighboring spins grow preferably parallel oriented. The surface fields in this region are stronger and thus capable of compensating the missing NN sites at the surfaces. But, since the fields on both surfaces have opposite orientations, one sees that, on the one hand, the field that has the same orientation as that of the dominant spin cluster will favor the growth of surface spins, while, on the other hand, the sites on the surface with opposite field will have a lower growing probability. Thus, on this disfavored side the growing interface becomes pinned and the curvature of the growing interface is not defined.

Keeping H fixed within Region II but increasing the temperature, thermal noise will enable the formation of drops on the disfavored side that eventually may nucleate

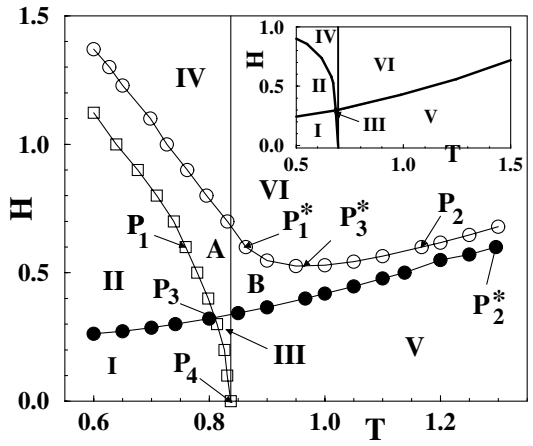

FIG. 2. H-T phase diagram corresponding to a lattice of size $L = 12$. The vertical straight line at $T_c(L) = 0.84$ corresponds to the L-dependent critical temperature [17], which separates the low-temperature ordered phase from the high-temperature disordered phase. Open (filled) circles refer to the transition between nondefined and concave (convex) growth regimes, and squares stand for the Ising-like localization-delocalization transition curve. Eight different regions are distinguished, as indicated in the figure. Also indicated are seven representative points that are discussed in the text. The inset shows the phase diagram corresponding to the thermodynamic limit composed of six different regions.

into larger clusters as the temperature is increased even further. This process may lead to the emergence of an up-down interface, separating oppositely oriented domains, running in the direction parallel to the walls. Since sites along the up-down interface are surrounded by oppositely oriented NN spins, they have a low growing probability. So, in this case the system grows preferably along the confinement walls and the growing interface is concave [Fig. 1(c)]. Then, as the temperature is increased, the system crosses to Region A (see Fig. 2) and we observe the onset of two competitive growth regimes: (i) one exhibiting a nondefined growing curvature that appears when a dominant spin orientation is present, as in the case shown in Fig. 1(b); (ii) another that appears when an up-down interface is established and the system has a concave growth interface, as is shown in Fig. 1(c).

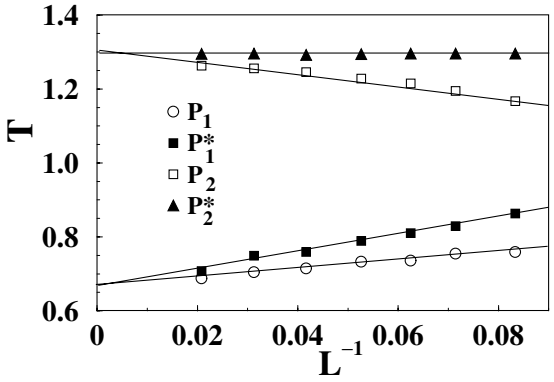

FIG. 3. Plots of T versus L^{-1} corresponding to the points P_1, P_1^*, P_2, and P_2^*, all of them with $H = 0.6$. The fits to the data (solid lines) show that $P_i \to P_i^*$ $(i = 1, 2)$ for $L \to \infty$.

Further increasing the temperature and for large enough fields, the formation of a stable longitudinal up-down interface that pushes back the growing interface is observed. So, the system adopts the concave growth regime [see Fig. 1(c) corresponding to Region IV in Fig. 2]. Increasing the temperature beyond $T_c(L)$, a transition from a low-temperature ordered state (Region IV) to a high-temperature disordered state [Region VI, see Fig. 1(e)], both within the concave growth regime, is observed. Analogously, for small enough fields, a temperature increase drives the system from the ordered convex growth regime (Region I) to the disordered convex growth regime [Region V, see Fig. 1(d)]. As shown in Fig. 2, there is also an intermediate fluctuating state (Region B) between Regions V and VI, characterized by the competition between the disordered convex growth regime and the disordered concave one.

Finally, a quite unstable and small region (Region III), that exhibits the interplay among the growth regimes of the contiguous regions, can also be identified. Since the width of Region III is of the order of the rounding observed in $T_c(L)$, large fluctuations between ordered and disordered states are observed, as well as from growth regimes of nondefined curvature to convex ones. However, Fig. 1(f) shows a snapshot configuration that is the fingerprint of Region III, that may prevail in the thermodynamic limit, namely, a well-defined spin up-down interface with an almost flat growing interface.

Let us now locate the transition curves between the already discussed regions. For this purpose, the mean transverse magnetization $m(k, L, T, H)$ is defined as

$$m(k, L, T, H) = \frac{1}{L^2} \sum_{i,j=1}^{L} S_{ijk}\,, \tag{2}$$

and the susceptibility (χ) is defined in terms of the magnetization fluctuations. Then, using a standard procedure [7], the localization-delocalization "transition" curve corresponding to the up-down interface running along the walls can be obtained considering that, on the H-T plane, a point with coordinates (H_w, T_w) on this curve maximizes $\chi(H, T)$. The obtained curve for the confined system is shown in Fig. 2. This localization-delocalization transition is also known as a prewetting transition and actually becomes a true wetting transition in the thermodynamic limit.

Since the MEM is a kinetic growth model, another kind of nonequilibrium wetting transition associated with the curvature of the growing interface can also be identified. In fact, varying the surface fields, one finds a transition between a wet state (that corresponds to a concave interface) and a nonwet state (associated with a convex interface), as already observed in Fig. 1. Clearly, two different contact angles must be defined in order to locate this transition,

namely, θ_D for the angle corresponding to the dominant spin cluster, and θ_{ND} for the one that corresponds to the nondominant spin cluster. Both contact angles can straightforwardly be determined by measuring the location of the growth interface averaged over a sufficiently long growing time. In this way, three different growth regimes can be distinguished: (i) the concave growth regime that occurs when the system wets the walls on both sides (i.e., for $\theta_D, \theta_{ND} < \frac{\pi}{2}$), (ii) the convex growth regime that occurs for $\theta_D, \theta_{ND} > \frac{\pi}{2}$, and (iii) the regime of nondefined curvature that occurs otherwise. The corresponding transition curves obtained for the confined system are shown in Fig. 2.

We will now extrapolate our results to show that the rich variety of phenomena found in a confined geometry is still present in the $L \to \infty$ limit, leading to the phase diagram shown in the inset of Fig. 2. In order to illustrate the extrapolation procedure, the following seven representative points of the finite-size phase diagram are discussed in detail: (i) the points labeled P_1, P_1^*, P_2, and P_2^*, that correspond to the intersections of the $H = 0.6$ line with the various transition curves shown in Fig. 2, and (ii) the points labeled P_3, P_3^*, and P_4, that refer to the intersection point between Regions I, II, III, and A, the minimum of the limiting curve between Regions IV–VI and A–B, and the zero-field transition point, respectively.

Figure 3 shows plots of T versus L^{-1} corresponding to the points P_1, P_1^*, P_2, and P_2^*. The results from the extrapolations are $T_1 = 0.67 \pm 0.01$, $T_1^* = 0.66 \pm 0.01$, and $T_2 = 1.30 \pm 0.02$, $T_2^* = 1.29 \pm 0.01$, pointing out that, within error bars, $P_i \to P_i^* (i = 1, 2)$ in the $L \to \infty$ limit. Using the same procedure, the extrapolations of P_3 and P_3^* (not shown here) give $H_3 = 0.30 \pm 0.01$, $H_3^* = 0.31 \pm 0.02$, and $T_3 = 0.69 \pm 0.01$, $T_3^* = 0.71 \pm 0.03$. So, one has $P_3 \to P_3^*$ for $L \to \infty$ within error bars. Finally, the extrapolation of P_4 is $T_4 = T_c = 0.69 \pm 0.01$.

Using the above-mentioned extrapolation procedure, the phase diagram in the thermodynamic limit can be drawn, as shown in the inset of Fig. 2. By comparison with the finite-size phase diagram of Fig. 2, notice that, besides the fact that the crossover Regions A and B vanish in this limit, it is expected that Region III may remain. Although this (very tiny) region corresponds to a physically well characterized growth regime, since one expects that the system in this region may grow in an ordered phase with a localized up-down domain interface and a convex growing interface, statistical errors due to large fluctuations close to criticality hinder the exact location of this region.

Comparing the equilibrium wetting phase diagram of the Ising model [3,6,7] and that of the MEM, it follows that the nonequilibrium nature of the latter introduces new and rich physical features of interest: The nonwet (wet) Ising phase splits out into Regions I and II (Regions III and IV), both within the ordered regime ($T < T_c$) but showing an additional transition in the interface growth mode. Also, the disordered state of the Ising system ($T > T_c$) splits out into Regions V and VI exhibiting a transition in the interface growth mode. The interplay between wetting of two interfaces, one of them defined between differently orientated domains that runs along the film, and the remaining one resulting from the growing process, leads to a multicritical wetting point close to $H^{MC} = 0.31 \pm 0.01, T^{MC} = 0.70 \pm 0.02$. At this particular multicritical point both interfaces are essentially perpendicular to each other [Fig. 1(f)].

We hope that the presented results will, on the one hand, contribute to the understanding of the rich and complex physical phenomena exhibited by the irreversible growth of binary mixtures in confined geometries, and, on the other hand, stimulate further experimental and theoretical work.

This work was supported by CONICET, UNLP, and ANPCyT (Argentina).

[1] M. E. Fisher and H. Nakanishi, J. Chem. Phys. **75**, 5857 (1981); **78**, 3279 (1983).
[2] S. Dietrich, in *Phase Transitions and Critical Phenomena,* edited by C. Domb and J. L. Lebowitz (Academic, New York, 1988), Vol. 12, p. 1.
[3] A. O. Parry and R. Evans, Phys. Rev. Lett. **64**, 439 (1990); Physica (Amsterdam) **181A**, 250 (1992).
[4] D. Urban, K. Topolski, and J. De Coninck, Phys. Rev. Lett. **76**, 4388 (1995).
[5] A. Díaz-Ortiz, J. M. Sánchez, and J. L. Morán-López, Phys. Rev. Lett. **81**, 1146 (1998).
[6] K. Binder, D. P. Landau, and A. M. Ferrenberg, Phys. Rev. Lett. **74**, 298 (1995); Phys. Rev. E **51**, 2823 (1995).
[7] E. V. Albano, K. Binder, D. W. Heermann, and W. Paul, Surf. Sci. **223**, 151 (1989).
[8] T. Kerle, J. Klein, and K. Binder, Phys. Rev. Lett. **77**, 1318 (1996); Eur. Phys. J. B **7**, 401 (1999).
[9] M. Mueller, K. Binder, and E. V. Albano, Europhys. Lett. **49**, 724 (2000).
[10] K. Binder, P. Nielaba, and V. Pereyra, Z. Phys. B **104**, 81 (1997).
[11] D. E. Sullivan and M. M. Telo Da Gama, *Fluid Interfacial Phenomena,* edited by C. A. Croxton (Wiley, New York, 1986).
[12] R. Evans and P. Tarazona, Phys. Rev. Lett. **52**, 557 (1984).
[13] From now on, we will unify the discussion in terms of a magnetic language. However, the relevant physical concepts can be extended to other systems such as fluids, polymers, and binary mixtures.
[14] H. Hinrichsen, R. Livi, D. Mukamel, and A. Politi, Phys. Rev. Lett. **79**, 2710 (1997).
[15] M. Ausloos, N. Vandewalle, and R. Cloots, Europhys. Lett. **24**, 629 (1993).
[16] J. Candia and E. V. Albano, Phys. Rev. E **63**, 066127 (2001).
[17] Among various definitions, $T_c(L)$ has been here identified with the peak of the susceptibility.